Available online at www.sciencedirect.com
ScienceDirect
Engineering Fracture Mechanics 74 (2007) 59–74
Engineering Fracture Mechanics
www.elsevier.com/locate/engfracmech

# Analytical study of the singularities arising at multi-material interfaces in 2D linear elastic problems

Alberto Carpinteri *, Marco Paggi

*Politecnico di Torino, Department of Structural Engineering and Geotechnics, Corso Duca degli Abruzzi 24, 10129 Torino, Italy*

Available online 20 March 2006

**Abstract**

The problem of stress singularities due to multi-material junctions in the material microstructure is addressed in the framework of the eigenfunction expansion method, provided that the eigenvalues are explicitly assumed complex. A novel efficient numerical procedure for computing the order of the stress singularity is presented. The numerical method can also be used to solve analogous singularity problems in anisotropic elasticity. According to this procedure, new problems of bi- and tri-material junctions occurring in the material microstructure are examined, paying special attention to the role played by Mode-I and Mode-II deformation. The effects of both the properties of the matrix and of the presence of transgranular cracks on the order of stress singularities are carefully investigated.


*Keywords:* Asymptotic analyses; Micromechanics and/or materials mechanics; Interface fracture; Transgranular fracture; Welded or bonded joints

## 1. Introduction

The problem of stress singularities in multi-material wedges and junctions has been deeply investigated in the Literature. Since the pioneering paper by Williams [1] about stress singularities in angular plates in extension, isotropic bi-material junctions [2–8], as well as isotropic tri- and *n*-material junctions [9–13] have been studied. More recently, singularity problems due to anisotropic multi-material wedges and junctions have been addressed (see [14–17], among others).

In the last few years, a renewed interest in singularity problems involving isotropic materials is emerged in order to detect and reduce singularities in the material mictrostructure. Engineering applications concern tri-material junctions at the grain boundaries in polycrystalline materials [18], microstructure of electronic devices [19] and junctions with an interphase inclusion [20]. Furthermore, it has been recently demonstrated that solutions for isotropic materials may also be gained by using the mathematical formalism of anisotropic elasticity applied to degenerate anisotropic materials (see [14,16,21], among others). Hence, in addition, solutions for

* Corresponding author. Tel.: +39 011 564 4850; fax: +39 011 564 4899.
*E-mail address:* alberto.carpinteri@polito.it (A. Carpinteri).

0013-7944/$ - see front matter 
doi:10.1016/j.engfracmech.2006.01.030

isotropic materials can be particularly useful when we are interested in checking the effectiveness of new approaches for anisotropic multi-material junctions by comparison with limit isotropic solutions [16].

In this paper, the general problem of isotropic multi-material junctions is addressed in the framework of the eigenfunction expansion method [1]. Then, a novel efficient numerical procedure for the computation of the eigenvalues is presented. It has to be remarked that this numerical method can be applied to any type of eigenvalue problem and it can also be used to find the roots of the eigenequations in anisotropic elasticity. Using this numerical procedure, solutions to new singularity problems in bi- and tri-material junctions are presented. These useful results can be used to characterize critical points for crack nucleation in the material microstructure. To this aim, a particular attention is devoted to the effect of the intermediate material, i.e. the matrix, and to the influence of transgranular cracks on the order of Mode-I and Mode-II stress singularities.

It has to be remarked that the obtained results strictly apply to 2D linear elastic problems. In the region of the singularity, the materials inevitably debond and the initial assumptions of linear elasticity may be violated. To characterize these problems, Sinclair [22] proposed to replace the traditional displacements continuity conditions along the interfaces with a cohesive stress-separation law. As a result, a number of configurations containing stress singularities according to the traditional asymptotic analysis become singularity-free. Nevertheless, from the engineering point of view, the introduction of these cohesive boundary conditions significantly increases the complexity of the analytical approach. Also, the use of cohesive models in the FE discretization framework can be very time consuming. To overcome these main drawbacks, Mohammed and Liechti [23] have recently proposed a simplified criterion for the prediction of the critical load for crack nucleation at bi-material corners. According to their model, the predicted failure loads for bi-material corners with an arbitrary corner angle can be computed as the failure load corresponding to a reference cracked bi-material specimen, obtained according to a nonlinear cohesive analysis, multiplied by a correction term which takes into account the real corner geometry. This correction term is a function of the order of the stress singularity computed according to the classical asymptotic analysis under the assumption of linear elasticity and perfect bonding. Therefore, it is expected that the results herein presented could be profitably used for future extensions of the formulation by Mohammed and Liechti to multi-material junction problems.

## 2. Mathematical formulation

The geometry of a plane elastostatic problem consisting of $n$ dissimilar isotropic, homogeneous wedges of arbitrary angles perfectly bonded along their interfaces which converge at the same vertex $O$ is depicted in Fig. 1. Each of the material regions is denoted by $\Omega_i$ with $i = 0, \ldots, n-1$, and it is comprised between the interfaces $\Gamma_i$ and $\Gamma_{i+1}$. The first and the last interfaces, corresponding respectively to $\theta = 0$ and $\theta = 2\pi$, coincide and are referred to as $\Gamma_0$.

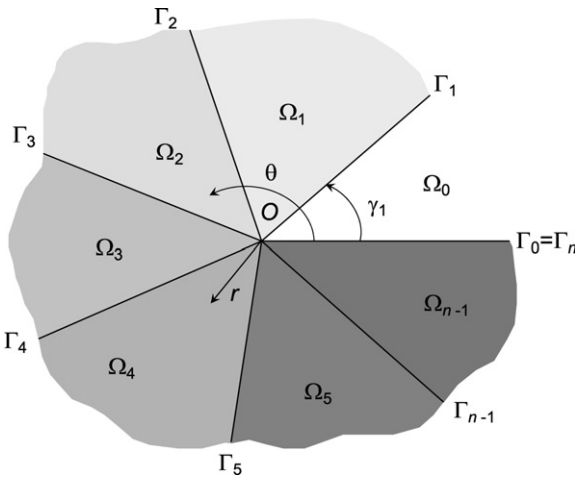


Fig. 1. Scheme of a multi-material junction.

According to Wieghardt [24] and to Williams [25], it is possible to assume, for the $i$th material region, the following separable form for the biharmonic stress function $\Phi_i$:

$$\Phi_i(r,\theta) = \sum_j r^{\lambda_j+1} f_{i,j}(\theta,\lambda_j), \tag{1}$$

where $\lambda_j$ and $f_{i,j}$ are referred to as eigenvalues and eigenfunctions, respectively. The summation with respect to the subscript $j$ is introduced in Eq. (1), since it is possible to have more than one eigenvalue for each problem and the Superposition Principle has to be applied. Stress and displacement fields are given by [1,26]:

$$\begin{aligned}
\sigma_r^i &= r^{\lambda-1}[f_i'' + (\lambda+1)f_i],\\
\sigma_\theta^i &= r^{\lambda-1}[\lambda(\lambda+1)f_i],\\
\tau_{r\theta}^i &= r^{\lambda-1}[-\lambda f_i'],\\
u_r^i &= \frac{r^\lambda}{2G_i}\left\{-(\lambda+1)f_i + \frac{1}{\lambda m_i}[f_i''' + (\lambda+1)^2 f_i]\right\},\\
u_\theta^i &= \frac{r^\lambda}{2G_i}\left\{-f_i' - \frac{1}{\lambda(\lambda-1)m_i}[f_i''' + (\lambda+1)^2 f_i']\right\},
\end{aligned} \tag{2}$$

where the constant $m$ depends on the Poisson's ratio and it is equal to $1+\nu_i$ for plane stress and to $1/(1-\nu_i)$ for plane strain. Parameter $G_i$ denotes the shear modulus of the $i$th material component.

Furthermore, the biharmonic condition requires $f_{i,j}$ to be of the following form:

$$f_{i,j} = A_{i,j}\sin[(\lambda_j+1)\theta] + B_{i,j}\cos[(\lambda_j+1)\theta] + C_{i,j}\sin[(\lambda_j-1)\theta] + D_{i,j}\cos[(\lambda_j-1)\theta], \tag{3}$$

where $A_{i,j}$, $B_{i,j}$, $C_{i,j}$ and $D_{i,j}$ are undetermined constants which have to be computed by enforcing boundary conditions.

### 2.1. Boundary conditions and eigenequations

Boundary conditions in case of perfect bonding are represented by stress and displacement continuity conditions along the $i$th interface:

$$\begin{aligned}
\sigma_\theta^i(r,\gamma_{i+1}) &= \sigma_\theta^{i+1}(r,\gamma_{i+1}),\\
\tau_{r\theta}^i(r,\gamma_{i+1}) &= \tau_{r\theta}^{i+1}(r,\gamma_{i+1}),\\
u_r^i(r,\gamma_{i+1}) &= u_r^{i+1}(r,\gamma_{i+1}),\\
u_\theta^i(r,\gamma_{i+1}) &= u_\theta^{i+1}(r,\gamma_{i+1})
\end{aligned} \tag{4}$$

paying attention to the fact that the interface $\Gamma_0$ has to be defined by $\gamma_0 = 0$ for region 1, and $\gamma_{n+1} = 2\pi$ for region $n$.

Furthermore, as argued by Chen and Nisitani [7], when the problem is characterized by a geometric symmetry, it is possible to subdivide the elastic field into a symmetric part and a skew-symmetric part, namely into a part due to the Mode-I deformation, and a part due to the Mode-II deformation. In the former case, the following symmetric conditions are applied at $\bar\theta = 0,\ \pi$, instead of Eq. (4):

$$\begin{aligned}
\tau_{r\theta}^i(r,\bar\theta) &= 0,\\
u_\theta^i(r,\bar\theta) &= 0.
\end{aligned} \tag{5}$$

In the latter, skew-symmetric conditions are imposed:

$$\begin{aligned}
\sigma_\theta^i(r,\bar\theta) &= 0,\\
u_r^i(r,\bar\theta) &= 0.
\end{aligned} \tag{6}$$

In this way, it is possible to study half a problem only and the total eigenequation is reduced to two factors: the former determines the eigenvalues corresponding to Mode-I deformation, whereas the latter determines the eigenvalues corresponding to Mode-II deformation.

Eventually, in case of either a re-entrant corner or a crack due to an imperfect bonding, traction-free conditions along the crack faces have to be considered in addition to continuity conditions of stresses and displacements (4) at interfaces:

$$\begin{aligned}&\sigma_\theta^i(r,\gamma_{i+1})=0,\\&\tau_{r\theta}^i(r,\gamma_{i+1})=0,\\&\sigma_\theta^{i+1}(r,\gamma_{i+1})=0,\\&\tau_{r\theta}^{i+1}(r,\gamma_{i+1})=0.\end{aligned}\tag{7}$$

To summarize, in case of perfect bonding without geometric symmetry in the problem, boundary conditions are represented by Eq. (4) only. On the other hand, if a geometric symmetry exists, then Eqs. (4)–(6) are considered. Eventually, in case of either a re-entrant corner or a crack, boundary conditions are given by Eq. (4) for the interfaces and by Eq. (7) for the crack faces. In matrix form, the equation set can be written as follows:

$$\mathbf{\Lambda v}=\mathbf{0},\tag{8}$$

where $\mathbf{\Lambda}$ denotes the coefficient matrix which non-linearly depends on the eigenvalue, and $\mathbf{v}$ represents the vector which collects the unknowns $A_{i,j}$, $B_{i,j}$, $C_{i,j}$ and $D_{i,j}$.

A nontrivial solution to the equation system (8) exists if and only if the determinant of the coefficient matrix vanishes. This condition yields to an eigenequation which has to be solved for eigenvalues which are in general complex. For the present purposes, we are concerned only with those values of $\lambda_j$ which may lead to singularities in the stress field. This fact, together with the condition of continuity of the displacement field at the vertex where regions meet, imply that we are seeking for eigenvalues in the range $0<\mathrm{Re}\,\lambda_j<1$. Then, to find solutions to the eigenequations, a numerical technique has to be employed.

### 2.2. Eigenfunctions

Once all the eigenvalues have been computed from the eigenequation, for each $\lambda_j$ we can express the unknowns in the $\mathbf{v}$ vector in terms of the first, say $A_1$. Then, the unknown constant $A_1$ is normalized such that the following expression for the stress field can be written:

$$\sigma^i=K_j r^{\lambda_j-1}f_{i,j}(\theta)+O(1),\tag{9}$$

where $O(1)$ indicates nonsingular terms. This procedure can be repeated for each $j$th eigenvalue, allowing to write an expression where all the eigenvalues contribute to the singular stress field near the vertex $O$:

$$\sigma^i=\sum_j K_j r^{\lambda_j-1}f_{i,j}(\theta)+O(1).\tag{10}$$

According to this method, stresses and displacements are determined to within a multiplicative constant which is referred to as *generalized stress-intensity factor* [13,27]. When the eigenvalues are complex, even the corresponding constants in the vector $\mathbf{v}$ are complex. Therefore, as pointed out by Pageau et al. [13], the direct application of Eq. (2) leads to stresses and displacements that are complex valued which, of course, are not valid. In these cases a valid solution can be obtained by considering the actual stresses and displacements as a linear combination of the complex stresses and displacements, respectively. Eventually, a particular attention has to be paid to materials and geometric configurations that correspond to the transition from two real roots to a complex conjugate pair. In these cases, nonseparable solutions exist and the eigenequations cannot be expressed as a function of the radial coordinate multiplied by a function of the angular coordinate [28]. Examples of these transitions were identified in tri-material junctions by Pageau et al. [10] and further cases will be shown in the sequel.

## 3. Numerical method for eigenvalues computation

For a given complex eigenvalue, let the value of the determinant of the coefficient matrix $\mathbf{\Lambda}$ in Eq. (8) be given by

$$\det\mathbf{\Lambda}=\mathrm{Re}(\det\mathbf{\Lambda})+\mathrm{iIm}(\det\mathbf{\Lambda}).\tag{11}$$

The values of $\lambda = \mathrm{Re}\,\lambda + \mathrm{i}\mathrm{Im}\,\lambda$ which cause the determinant of the coefficient matrix to be zero are the eigenvalues of the problem. In practice, the problem consists in finding the real and the imaginary parts of $\lambda$ such that $\mathrm{Re}(\det\mathbf{\Lambda}) = \mathrm{Im}(\det\mathbf{\Lambda}) = 0$.

Carpenter and Byers [29] set up a numerical procedure based on the computation of the determinant (11) and the subsequent plot of the contour lines of $\mathrm{Re}(\det\mathbf{\Lambda}) = 0$ and $\mathrm{Im}(\det\mathbf{\Lambda}) = 0$. Intersection of the $\mathrm{Re}(\det\mathbf{\Lambda}) = 0$ and $\mathrm{Im}(\det\mathbf{\Lambda}) = 0$ contour lines yields the desired eigenvalues. A direct inspection of this contour plot permits to obtain tentative values for the eigenvalues that are subsequently used as estimates for the Muller's algorithm [30,31] which returns refined eigenvalues. This procedure was employed in order not to miss eigenvalues, which is a typical problem with eigenvalue solution routines. The same algorithm was also recently adopted by Cheng [15] and by Barroso et al. [16], among others, for the computation of the singularities in anisotropic multi-material junctions.

Dempsey and Sinclair [32] developed systematic methods of expansion and simplification of the determinant, e.g. the expansion by complementary minors and the transfer matrix approach. In any case, numerical procedures usually employed [15,16,26] are based on a direct evaluation of the determinant of the coefficient matrix and a subsequent research of the zeros of the eigenequations.

It is well-known that, from the numerical point of view, the computation of the determinant of a matrix is a nonconvenient procedure in terms of both the accuracy of the solution and the number of operations [33]. Hence, an efficient numerical method which permits to compute the eigenvalues without working out the determinant of the coefficient matrix is herein proposed. To this aim, let us define the condition number of the square matrix $\mathbf{\Lambda}$ [33]:

$$\mathrm{cond}(\mathbf{\Lambda}) := \|\mathbf{\Lambda}\|\|\mathbf{\Lambda}^{-1}\|, \tag{12}$$

where $\|\cdot\|$ is any valid matrix norm. The condition number is a measure of stability or sensitivity of a matrix (or the corresponding linear system) to numerical operations.

Matrices with condition numbers near the unity are said to be *well-conditioned*. Matrices with condition numbers much greater than one (such as $10^5$ for a $5\times 5$ Hilbert matrix) are said to be *ill-conditioned*. One of the major properties of the condition number is that, if $\mathrm{cond}(\mathbf{\Lambda})$ is the condition number of $\mathbf{\Lambda}$ in the $p$-norm, then it can be used as a measure of the relative $p$-norm distance from the set of singular matrices:

$$\frac{1}{\mathrm{cond}(\mathbf{\Lambda})} := \min\left\{\frac{\|\mathbf{\Lambda}-\mathbf{S}\|}{\|\mathbf{S}\|} : \mathbf{S}\in\mathbb{C}^{4n\times 4n} \text{ singular}\right\}, \tag{13}$$

where the matrices $\mathbf{S}$ pertain to a subset of the matrices $\mathbf{\Lambda}$ such that their determinant is equal to zero. In the range $0 < \mathrm{Re}\,\lambda < 1$ it is possible to find out more than one singular matrix. Therefore, the numerical algorithm for determining the eigenvalues can be stated as follows:

(1) compute the condition number according to an efficient subroutine (see [34] for more details about numerical procedures), for several values of the real and the imaginary parts of $\lambda$, with $0 < \mathrm{Re}\,\lambda < 1$;
(2) plot $\mathrm{cond}(\mathbf{\Lambda})$ vs. $\mathrm{Re}\,\lambda$ and $\mathrm{Im}\,\lambda$;
(3) the eigenvalues correspond to the maxima of $\mathrm{cond}(\mathbf{\Lambda})$, i.e. to the values of $\lambda$ yielding to ill-conditioned or singular matrices.

To show the effectiveness of the above-described numerical procedure, some illustrative examples are presented. First of all, let us consider an isotropic bi-material junction with material 2 occupying a quarter plane region. It is well-known that the eigenvalues for perfectly bonded bi-material junctions are real [7]. A mechanical configuration characterized by plane strain conditions with $E_2/E_1 = 0.001$ and $\nu_1 = \nu_2 = 0.2$ is addressed. Hence, the eigenfunction is depicted in Fig. 2(a) vs. the real part of $\lambda$. The condition number is less than 20 when the matrix is nonsingular, suggesting that the matrix is substantially well-conditioned. On the other hand, for the eigenvalues of the problem corresponding to a vanishing eigenequation, the condition number increases up to $10^8$, i.e. it is 7 orders of magnitude higher than that for singular matrices. These jumps in the values of $\mathrm{cond}(\mathbf{\Lambda})$ can be readily seen in Fig. 2(b), where the condition number is plotted vs. $\mathrm{Re}\,\lambda$. Due to the

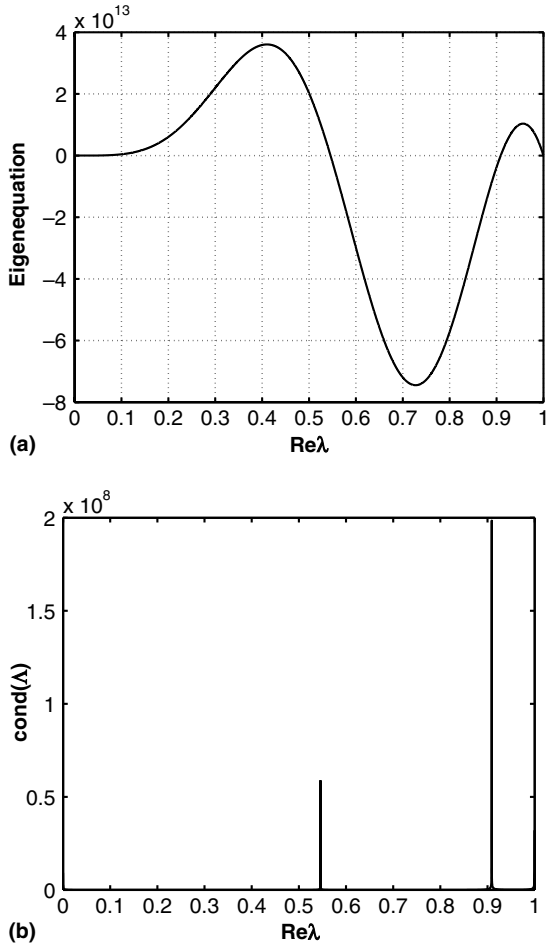


Fig. 2. (a) Eigenequation and (b) condition number as functions of the real part of the eigenvalue for a bi-material junction with material 2 occupying a quarter plane region with $E_2/E_1 = 0.001$ and $\nu_1 = \nu_2 = 0.2$ (plane strain).

difference of 7 orders of magnitude, the condition number for nonsingular matrices looks like zero in this diagram.

Another bi-material problem with the same geometry and characterized by plane strain conditions with $E_2/E_1 = 10$ and $\nu_1 = \nu_2 = 0.2$ is also addressed. The eigenequation and the condition number vs. $\mathrm{Re}\,\lambda$ are depicted in Fig. 3(a) and (b), respectively. In this case, the roots of the eigenequation are close to each other. Hence, this problem is particularly difficult to handle with a traditional numerical method for the computation of the zeros of equations. On the contrary, high values of the condition number are correctly predicted by the proposed method in correspondence of the two real eigenvalues of the problem.

The last example concerns a perfectly bonded isotropic tri-material junction with materials 1 and 2 occupying two adjacent quarter plane regions. Mechanical parameters are: $E_2/E_1 = 10{,}000$, $E_3/E_1 = 10$ and $\nu_1 = \nu_2 = \nu_3 = 0.2$ in plane strain condition (see Fig. 11 in [10] for the evolution of the order of the stress singularity in terms of the elastic mismatch). In this case the eigenvalue is complex and the solution of the problem corresponds to $\lambda$ such that both $\mathrm{Re}(\det \mathbf{\Lambda})$ and $\mathrm{Im}(\det \mathbf{\Lambda})$ are equal to zero. The numerical procedure based on the evaluation of the condition number is particularly effective also for this problem, since the eigenvalues are simply given by the coordinates of the maxima of the condition number in the $\mathrm{Re}\,\lambda$–$\mathrm{Im}\,\lambda$ plane. The contour plot and the three-dimensional plot of the condition number are depicted, respectively, in Fig. 4(a) and (b). From these diagrams, the real and imaginary parts of the eigenvalue can be easily determined.

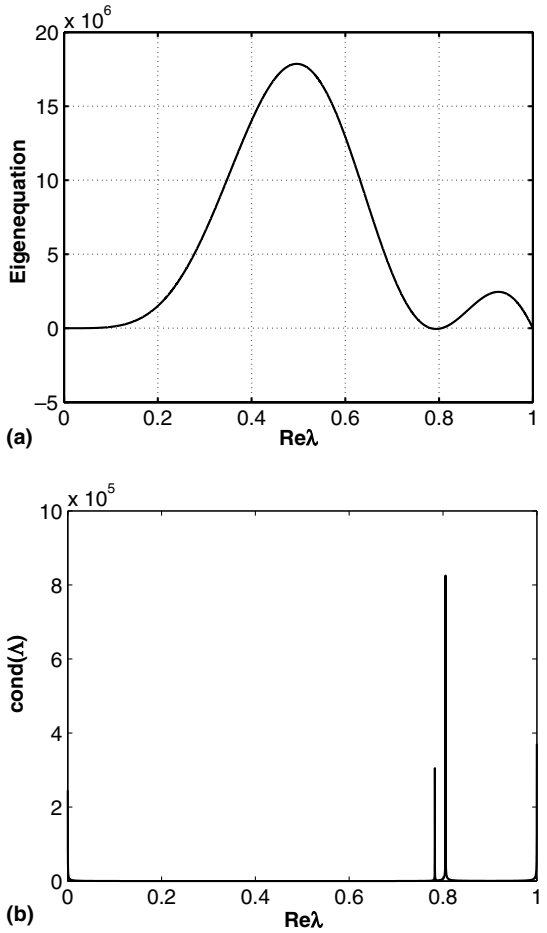


Fig. 3. (a) Eigenequation and (b) condition number as functions of the real part of the eigenvalue for a bi-material junction with material 2 occupying a quarter plane region with $E_2/E_1 = 10$ and $v_1 = v_2 = 0.2$ (plane strain).

## 4. Numerical examples of singularities due to bi- and tri-material junctions

### 4.1. Perfectly bonded material junctions

Two configurations of bi-material junctions with perfectly bonded interfaces whose schemes are depicted in Fig. 5(a) and (b) are addressed. Computed eigenvalues are presented in Figs. 6 and 8 for several values of the ratio between the elastic moduli of the two materials. Solutions can also be expressed in terms of Dundurs' constants [35,36]. However, some of the subsequent solutions herein developed cannot be expressed in terms of these constants and, therefore, they are not introduced here. Angular positions of the interfaces are also indicated in the schemes of Fig. 5.

The problem in Fig. 5(a) was firstly addressed by Bogy and Wang [5] by using the Mellin transform technique. In that study, the minimum eigenvalue only was computed. Then, Chen and Nisitani [7] derived Mode-I and Mode-II eigenvalues according to the Muskhelishvili complex function representation for some geometrical and material parameters. For this case, two real roots greater than 0.5 exist for each value of the modular ratio $E_2/E_1$. For $E_2/E_1$ approximately less than 10.0, the minimum eigenvalue is due to Mode-I deformation, whereas, for modular ratios greater than that value, this trend is inverted and the eigenvalues due to Mode-II deformation are less than those due to Mode-I (see Fig. 6).

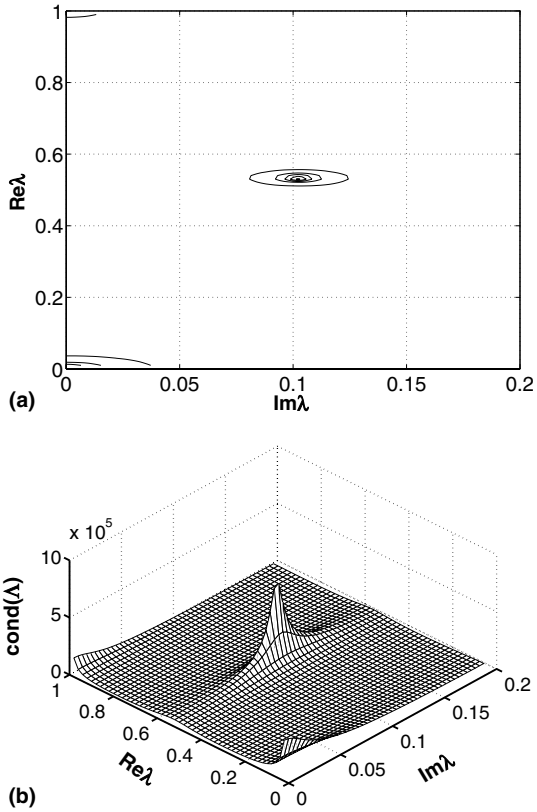


Fig. 4. (a) Contour plot and (b) three-dimensional graph of the condition number as a function of the real and the imaginary parts of the eigenvalue for a tri-material junction with materials 1 and 2 occupying two adjacent quarter plane regions. Mechanical parameters are: $E_2/E_1 = 10{,}000$, $E_3/E_1 = 10$ and $v_1 = v_2 = v_3 = 0.2$ (plane strain).

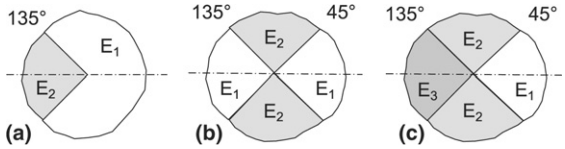


Fig. 5. Schemes of bi- and tri-material junctions herein considered.

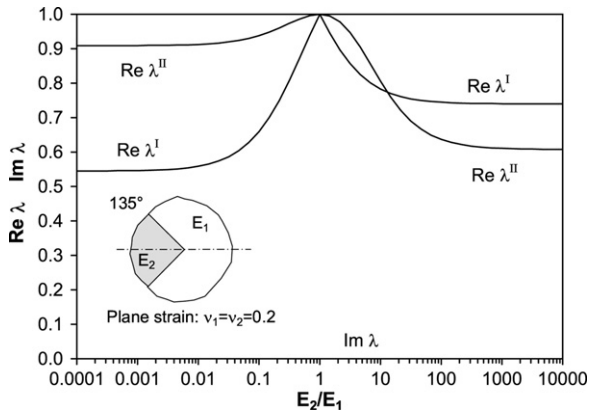


Fig. 6. Mode-I and Mode-II eigenvalues for the bi-material junction of Fig. 5(a).

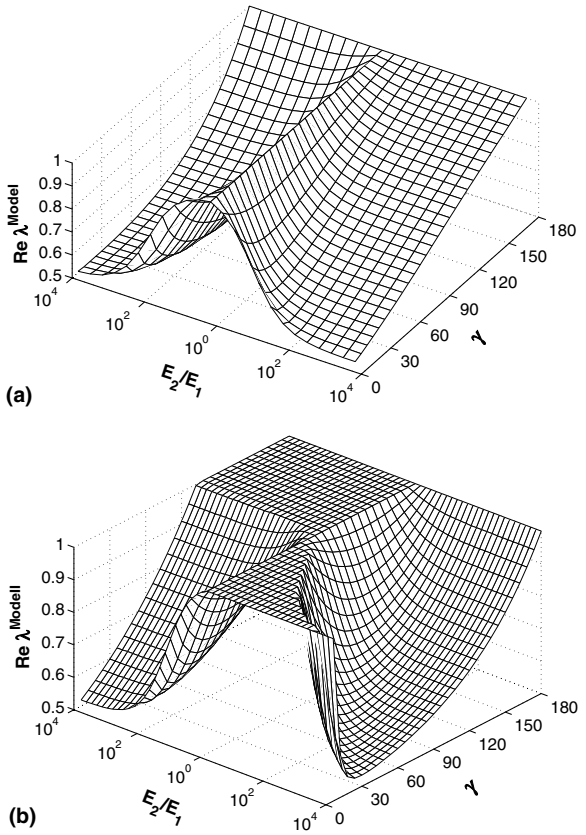


Fig. 7. (a) Mode-I and (b) Mode-II eigenvalues for the bi-material junction of Fig. 5(a) in case of several geometric and material combinations.

As argued by Chen and Nisitani [7], this result implies that the simple form $\sigma \sim r^{\min(\mathrm{Re}\,\lambda)-1}$ for the singular stress field holds only in case of Mixed-Mode deformation, while in either Mode-I or Mode-II only, $\min(\mathrm{Re}\,\lambda)$ has to be replaced with $\min(\mathrm{Re}\,\lambda^{\mathrm{I}})$ or $\min(\mathrm{Re}\,\lambda^{\mathrm{II}})$, respectively. When the two materials present the same elastic moduli, i.e. $E_2/E_1 = 1$, $\mathrm{Re}\,\lambda$ is equal to 1.0 and the stress singularity disappears.

Computed eigenvalues presented in Fig. 7 are a completion of this problem, since the eigenvalues are depicted as functions of both the elastic modular ratio, $E_2/E_1$, and of the wedge angle, $\gamma$, of material 2. These new useful diagrams clearly permit to find optimum geometrical and mechanical configurations with a vanishing singularity. Results in the range $\pi < \gamma < 2\pi$ can be simply obtained by symmetry. For any configuration, two real roots greater than 0.5 exist. From the engineering point of view, it is important to notice that, in case of Mode-II deformation, there are several mechanical and geometrical configurations for which no eigenvalues are found with vanishing singularities.

Furthermore, the limit problems of $\gamma \to 0$ with either an infinitely stiff or an extremely soft material 2 require a special attention. These problems correspond, respectively, to a crack with either clamped or stress-free surfaces inside a homogeneous material. Theoretical solutions provide $\mathrm{Re}\,\lambda = 0.5$ for both Mode-I and Mode-II deformation [1]. Interestingly, in Fig. 7(b) it seems that $Re\,\lambda^{\mathrm{II}} \to 1$ when $\gamma \to 0$ and $E_2/E_1 \to 1 \times 10^4$. This unexpected behavior can be explained by observing that, if a geometrical configuration characterized by $\gamma = 2^\circ$ is considered, no stress singularities are found for modular ratios up to approximately $E_2/E_1 = 1 \times 10^6$. Therefore, the considered range of $E_2/E_1$ in Fig. 7(b) is not large enough to exhibit this limit behavior for a crack with perfectly clamped boundary conditions which can be achieved for $E_2/E_1 \to \infty$.

The latter bi-material problem presented in Fig. 5(b) has, to best of our knowledge, not yet been studied before. Eigenvalues less than 0.5 exist (see Fig. 8), i.e. super-singularities are found. The stress singularity becomes the strongest, i.e. $\mathrm{Re}\,\lambda \to 0$, for either a very stiff or a very soft material 2. The symmetry of the

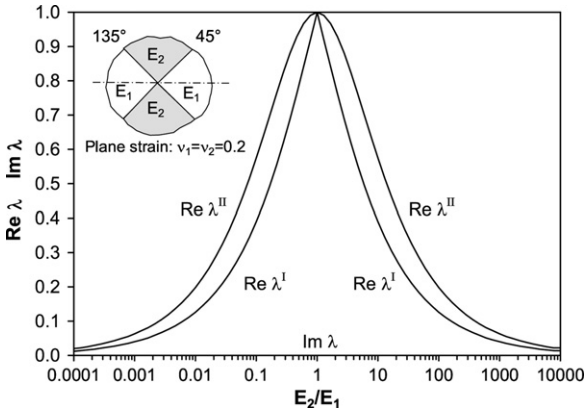


Fig. 8. Mode-I and Mode-II eigenvalues for the bi-material junction of Fig. 5(b) with perfectly bonded interfaces.

solution with respect to $E_2/E_1 = 1$ is due to the double geometric symmetry of the problem with respect to horizontal and vertical axes. For this case, the singularity disappears only for the trivial case of $E_2/E_1 = 1$ and $\mathrm{Re}\,\lambda^{\mathrm{I}}$ is always less than $\mathrm{Re}\,\lambda^{\mathrm{II}}$.

In the problem schematically depicted in Fig. 5(c), two materials occupying two quarter planes with a specified ratio between their elastic moduli $E_3/E_1$ are joined by an intermediate material whose elastic modulus $E_2$ is varied from $E_1$ to $E_3$. This configuration can be observed in the microstructure of polycrystalline materials with material 2 as a matrix in which grains with different elastic parameters are embedded. Different mechanical configurations characterized by the ratio $E_3/E_1$ are considered. The limit case given by $E_3/E_1 = 1$ corresponds to a bi-material junction whose eigenvalues are depicted in Fig. 8.

Solutions to tri-material junctions characterized by $E_3/E_1 = 100$ and $E_3/E_1 = 10{,}000$ are depicted, respectively, in Fig. 9(a) and (b). For such problems, the limit cases given by either $E_2/E_1 = 1$ or $E_2/E_1 = E_3/E_1$ correspond to bi-material junctions whose eigenvalues are shown in Fig. 6. Thanks to the geometric symmetry of these problems, the roots of the eigenequations corresponding to either Mode-I or Mode-II deformation can be separately computed. It is interesting to notice that, regardless of the value of the elastic modular ratio $E_3/E_1$, there are some mechanical configurations admitting only one root of the eigenequation (see Fig. 9(a) and (b)). To be more specific, when the elastic modulus of the intermediate material is close to that of the softer component, no stress singularities due to Mode-I deformation are found. On the other hand, when the Young's modulus of the intermediate material approaches that of the third material, Mode-II stress singularities are avoided. These trends are completely general for this type of tri-material junction and can be observed for any given value of the parameter $E_3/E_1$ different from 1.

In case of Mixed-Mode deformation, the minimum singularity criterion [10] would suggest that the more suitable material configuration is attained for the case corresponding to the maximum eigenvalues. As a consequence, for such tri-material junction problems the optimum configuration would correspond to a stiffness ratio such that $\mathrm{Re}\,\lambda^{\mathrm{I}} = \mathrm{Re}\,\lambda^{\mathrm{II}}$ (see Fig. 9). By considering tri-material junctions with different values of the ratio $E_3/E_1$, the value of $E_2/E_1$ is computed according to the above criterion and depicted in Fig. 10 vs. the ratio between the elastic moduli of materials 1 and 3. From these results, the following regression curve is obtained:

$$E_2/E_1 = 0.933(E_3/E_1)^{0.467} \cong \sqrt{E_3/E_1}. \tag{14}$$

In practice, this condition rules out intermediate materials whose elastic moduli are close to that of the stiffer material. Furthermore, it is important to notice that all the roots are necessary to describe the stress state in both materials. It cannot be concluded that any root is somehow less dominant.

### 4.2. Junctions with transgranular cracks

Debonding along interfaces in tri-material junctions have been considered by Pageau et al. [10], whereas a little attention has been devoted in the Literature to the problem of cracks inside the material regions. Hence,

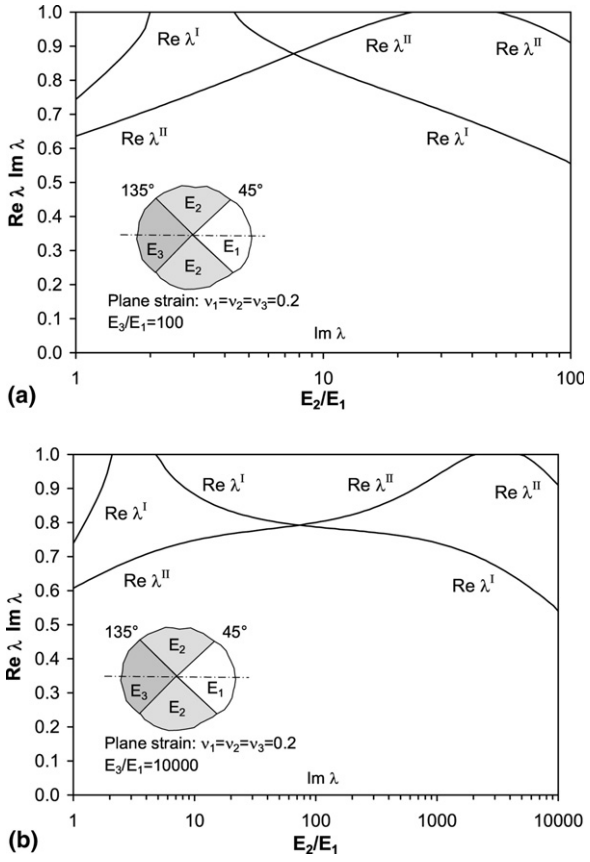


Fig. 9. Eigenvalues for the tri-material junction of Fig. 5(c) with perfectly bonded interfaces and (a) $E_3/E_1 = 100$ and (b) $E_3/E_1 = 10{,}000$.

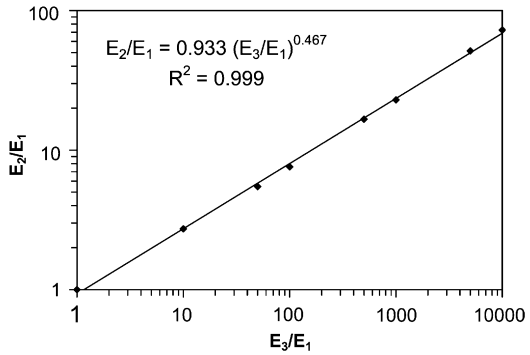


Fig. 10. Relation between $E_2/E_1$ and $E_3/E_1$ according to the minimum singularity criterion.

some of the previous results related to the order of the stress singularity are extended to the case when a crack is introduced along the symmetry line (see also the schemes in Fig. 11).

The computed eigenvalues for the problem in Fig. 11 (b) are presented in Fig. 12 and match exactly the well-known solution provided by Zak and Williams [2]. Roots of the eigenequations are real for each value of the ratio $E_2/E_1$ and the eigenvalues due to Mode-I and Mode-II coincide. Analogously to the problem of Fig. 5(b), the singularity becomes the strongest, i.e. $\mathrm{Re}\,\lambda \to 0$, when $E_2/E_1 \to \infty$ and the two portions of material 2 are joined by an extremely soft material.

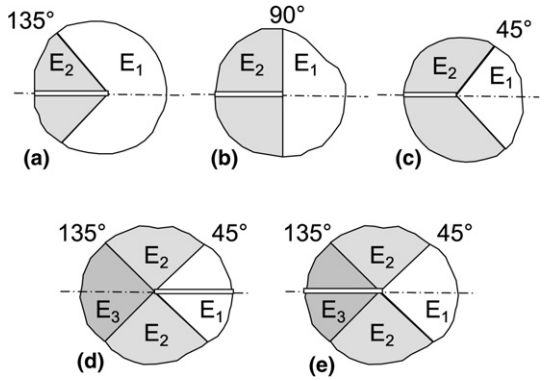


Fig. 11. Schemes of bi- and tri-material junctions with a crack herein considered.

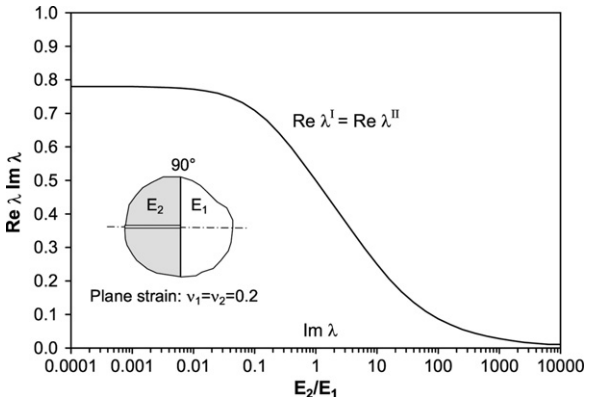


Fig. 12. Eigenvalues for the bi-material junction with a crack of Fig. 11 (b).

Furthermore, when $E_2/E_1 = 1$, $\mathrm{Re}\,\lambda$ is equal to 0.5, it being the well-known eigenvalue for a crack in a homogeneous medium. For this problem, no singularities occur in the fully bonded case. Varying the position of the interface, it is possible to generalize the study proposed by Zak and Williams [2] to other geometric configurations. Then, the eigenvalues for the two cases corresponding to the interface at 135° and 45° are depicted in Fig. 13(a) and (b), respectively.

These problems were also partially addressed by Inoue and Koguchi [12]. They computed the eigenvalues according to the Mellin transform technique and plotted the minimum eigenvalues only for the case of $\gamma = 120°$. No attention was paid neither to Mode-I and Mode-II singularities, nor to the cases in which the wedge angle of material 2 is greater than 120°.

Results of fully bonded conditions are also reported with dashed lines in Fig. 13. In the former configuration, Mode-I and Mode-II eigenvalues are not the same and four real roots are found. When the mechanical mismatch disappears, i.e. for $E_2/E_1 = 1$, eigenvalues due to Mode-I and to Mode-II are equal to 0.5. For values of the ratio between the elastic moduli $E_2/E_1$ less than 1.0, $\min(\mathrm{Re}\,\lambda^{\mathrm{I}})$ is less than $\min(\mathrm{Re}\,\lambda^{\mathrm{II}})$, whereas an opposite behavior occurs for the other material combinations. In the latter case (see Fig. 13(b)), two complex roots appear for values of $E_2/E_1$ approximately less than 0.1. Also in this case, when the elastic mismatch disappears, two coincident eigenvalues equal to 0.5 are found.

Comparison of the two-material results for the cracked and uncracked cases in Fig. 13(a) and (b) shows a rather interesting trend. When material 2 containing the crack is much less stiff than material 1, the roots are very similar to those of the uncracked configurations. For values of $E_2/E_1$ greater than unity, stress singularities for the cracked cases become quickly more severe than those corresponding to the fully bonded problems. When the ratio $E_2/E_1$ tends to infinity, $\mathrm{Re}\,\lambda$ approaches 0 and the order of the singularity tends to the unity,

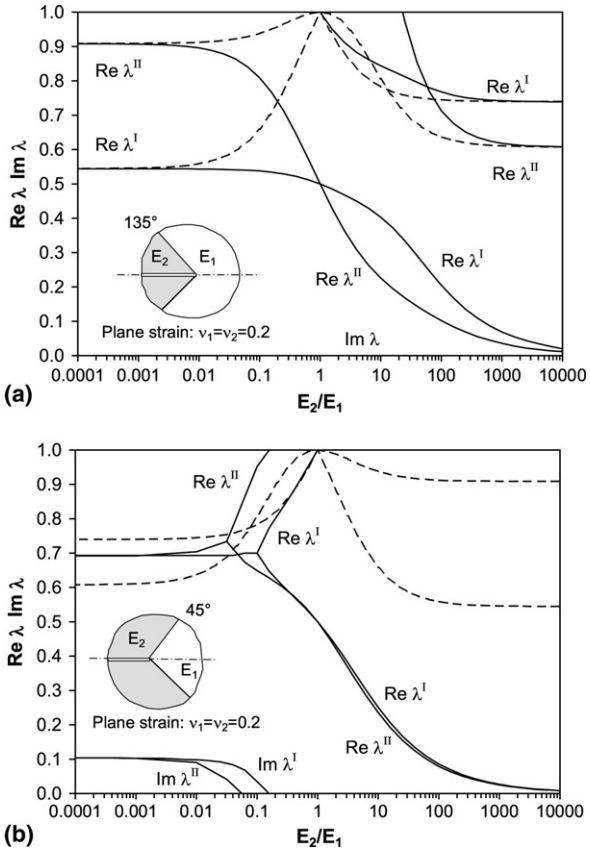


Fig. 13. Eigenvalues for the bi-material junction with a crack of (a) Fig. 11(a) and (b) Fig. 11(c).

i.e. the stresses vary like $1/r$ for small values of $r$. In any case, all the roots are necessary to describe the stress state in both materials.

From the engineering point of view, a criterion of minimum singularity would suggest that, regardless of the geometric configuration, a crack in the stiffer material can be very dangerous. For instance, it is possible that in Mixed-Mode deformation the propagation of the intragranular crack could be enhanced, quickly leading to a debonding along the interfaces or a crack penetration in the softer material. This is also true for ratios of the elastic moduli in the range $1 < E_2/E_1 < 10$, very common to observe in many engineering applications.

Eigenvalues in Fig. 14(a) and (b) represent a direct extension to tri-material junctions of the above results for cracked bi-material junctions. As a representative case, let us consider the uncracked problem analyzed in Fig. 9(a) characterized by $E_3/E_1 = 100$. The Young's modulus of the intermediate material is the independent variable of the problem and it is varied from $E_1$ to $E_3$. A crack is then considered either in the softer or in the stiffer material. For each case study, real and imaginary parts of Mode-I and Mode-II eigenvalues are computed.

As a limit case, when the crack lies in the softer material (see Fig. 14(a)) and $E_2/E_1 = 1$, the problem reduces to the cracked bi-material junction with $E_2/E_1 = 1/100$ whose eigenvalues are also shown in Fig. 13(b). Analogously, when the tri-material junction is characterized by $E_2/E_1 = 100$, we have the bi-material problem whose roots are provided in Fig. 13(a) for $E_2/E_1 = 1/100$. The same reasoning holds when the crack lies in the stiffer material (see Fig. 14(b)) and the limit cases of $E_2/E_1 = 1$ and $E_2/E_1 = 100$ are addressed. For a direct comparison between cracked and uncracked solutions, eigenvalues for the corresponding uncracked problems are depicted with dashed lines in Fig. 14.

When the crack lies in the softer material (see Fig. 14(a)), Mode-I and Mode-II eigenvalues remain greater than 0.5, as in the uncracked problem. The main difference is represented by the fact that in the range

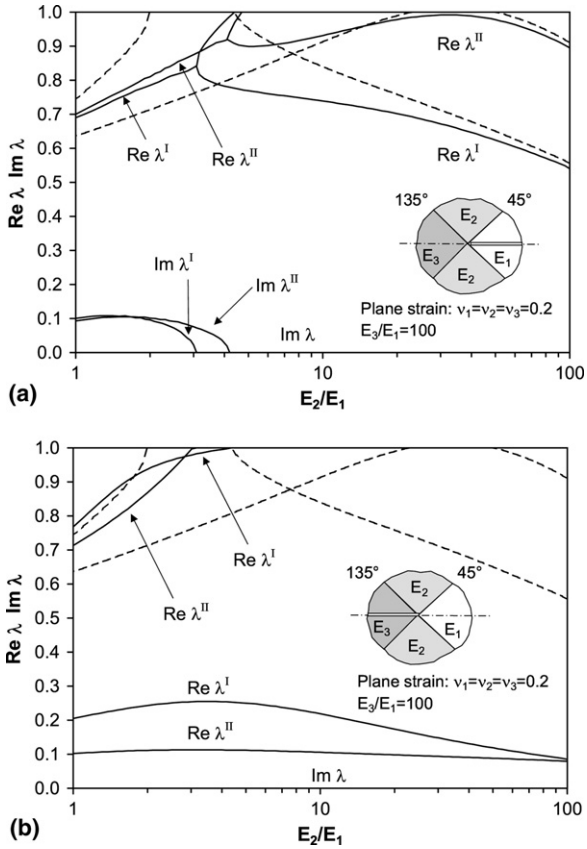


Fig. 14. Eigenvalues for the tri-material junction with a crack of (a) Fig. 12(d) and (b) Fig. 12(e).

$3 < E_2/E_1 < 4$, Mode-II eigenvalues are complex and two real roots are found for Mode-I deformation. Furthermore, for $E_2/E_1$ approximately equal to 3, a transition from two real roots to a complex conjugate pair also occurs for Mode-I eigenvalues. On the other hand, a completely different behavior has to be noticed for a crack in the stiffer material (see Fig. 14(b)). Computed eigenvalues for this problem are real and two additional roots are found in the range $1 < E_2/E_1 < 4$ with respect to the uncracked configurations. Such roots are far lower than 0.5, i.e. the corresponding order of the stress singularity is more severe than that due to a crack inside a homogeneous material. For $E_2/E_1 > 4$, the eigenvalues greater than 0.5 disappear and the stress state is characterized by the lower roots only.

As also observed for cracked bi-material junctions, these results imply that the asymptotic behavior of the singular stress field can be strongly influenced by cracks inside the stiffer material. Bi- and tri-material junctions between sharp aggregates are commonly observed in the microstructure of concrete composites [37]. In normal strength concrete the weakness of the interface inhibits the achievement of transgranular fracture. On the other hand, in high-strength concrete, it is more likely to have cracks penetrating the aggregate particles and in these cases the role of the aggregate phase, crack-aggregate and mortar-aggregate interactions are currently under investigation [38,39]. We suggest that results concerning the super-singular behavior of transgranular cracks may be a possible reason of the less pronounced effect of crack arrest by aggregates and a more brittle global behavior in high-strength concrete, as experimentally observed in [40].

## 5. Conclusions

In the present paper, the formulation of the general problem of multi-material junctions was provided according to the mathematical formalism of the eigenfunction expansion method. An efficient numerical pro-

cedure to compute the order of the stress singularity was presented. We point out that this procedure can be also applied to analogous problems in anisotropic elasticity.

Numerical results concerning bi- and tri-material junctions perfectly bonded along their interfaces are obtained. Materials are linear elastic, isotropic and in a condition of plane stress or plane strain. Thanks to the geometric symmetry of the problems, singularities due to either Mode-I or Mode-II deformation are separated.

From the engineering point of view, the obtained results provide useful information about the variation of the order of the stress singularity when the stiffness of one material varies with respect to the others. Contrarily to the results obtained by Pageau et al. [10], suggesting that an intermediate material increases the order of the stress singularity in tri-material junction geometries when one material occupies a half plane region, we have shown that a third material can be favorable for the tri-material junctions herein investigated. The criterion of minimum singularity suggests that the best choice is given by an intermediate material, i.e. a matrix, whose elastic modulus is closer to that of the softer component.

Eventually, results concerning cracked geometries demonstrate that both bi- and tri-material junctions can be significantly influenced by cracks in the stiffer material. This result can be a possible explanation to the more brittle global behavior of high-strength concrete where transgranular cracks may occur.

Numerical results show that all the eigenvalues must be taken into account for an accurate elastic stress analysis. From the numerical point of view, the results of this study can be profitably used to define generalized singular finite elements for the direct numerical determination of generalized stress-intensity factors [41].

## Acknowledgements

Support of the Italian Ministry of University and Research (MIUR) is gratefully acknowledged.

## References

[1] Williams ML. Stress singularities resulting from various boundary conditions in angular corners of plates in extension. ASME J Appl Mech 1952;74:526–8.
[2] Zak AR, Williams ML. Crack point stress singularities at a bi-material interface. ASME J Appl Mech 1963;30:142–3.
[3] Bogy DB. Two edge-bonded elastic wedges of different materials and wedge angles under surface tractions. ASME J Appl Mech 1971;38:377–86.
[4] Hein VL, Erdogan F. Stress singularities in a two-material wedge. Int J Fract Mech 1971;7:317–30.
[5] Bogy DB, Wang KC. Stress singularities at interface corners in bonded dissimilar isotropic elastic materials. Int J Solids Struct 1971;7:993–1005.
[6] Dempsey JP, Sinclair GB. On the singular behaviour of a bi-material wedge. J Elasticity 1981;11:317–27.
[7] Chen D, Nisitani H. Singular stress field near the corner of jointed dissimilar materials. ASME J Appl Mech 1993;60:607–13.
[8] Munz D, Yang YY. Stress singularities at the interface in bonded dissimilar materials under mechanical and thermal loading. ASME J Appl Mech 1992;59:857–61.
[9] Theocaris PS. The order of singularity at a multi-wedge corner of a composite plate. Int J Engng Sci 1974;12:107–20.
[10] Pageau SS, Joseph PF, Biggers Jr SB. The order of stress singularities for bonded and disbonded three-material junctions. ASME J Appl Mech 1994;31:2979–97.
[11] Pageau SS, Joseph PF, Biggers Jr SB. Singular antiplane stress fields for bonded and disbonded three-material junctions. Engng Fract Mech 1995;52:821–32.
[12] Inoue T, Koguchi H. Influence of the intermediate material on the order of stress singularity in three-phase bonded structure. Int J Solids Struct 1996;33:399–417.
[13] Pageau SS, Gadi KS, Biggers Jr SB, Joseph PF. Standardized complex and logarithmic eigensolutions for n-material wedges and junctions. Int J Fract 1996;77:51–76.
[14] Desmorat R, Leckie FA. Singularities in bi-material: parametric study of an isotropic/anisotropic joint. Eur J Mech, A/Solids 1998;17:33–52.
[15] Chen H-P. Stress singularities in anisotropic multi-material wedges and junctions. Int J Solids Struct 1998;35:1057–73.
[16] Barroso A, Mantič V, París F. Singularity analysis of anisotropic multimaterial corners. Int J Fract 2003;119:1–23.
[17] Chue C-H, Weng S-M. Stress singularities in anisotropic three-material wedges and junctions with applications. Compos Struct 2002;58:443–56.
[18] Picu CR, Gupta V. Stress singularities at triple junctions with freely sliding grains. Int J Mech Phys Solids 1996;33:1535–41.
[19] Liu XH, Suo Z, Ma Q. Split singularities: stress field near the edge of a silicon die on a polymer substrate. Acta Mater 1999;47:67–76.
[20] Boniface V, Simha KRY. Suppression of complex singularity using wedge interphase in interface fracture. Int J Solids Struct 2001;38:5411–20.

[21] Choi ST, Shin H, Earmme YY. On the unified approach to anisotropic and isotropic elasticity for singularity, interface and crack in dissimilar media. Int J Solids Struct 2003;40:1411–31.
[22] Sinclair GB. On the influence of cohesive stress-separation laws on elastic stress singularities. J Elasticity 1996;44:203–21.
[23] Mohammed I, Liechti KM. Cohesive zone modeling of crack nucleation at bimaterial corners. J Mech Phys Solids 2000;48:753–64.
[24] Wieghardt K. Über das spalten und zerreissen elastischer körper. Z. Math Physik 1907;55:60–103.
[25] Williams ML. The stress around a fault or crack in dissimilar media. Bull Seismol Soc Am 1959;49:199–204.
[26] Fenner DN. Stress singularities in composite materials with an arbitrarily oriented crack meeting an interface. Int J Fract 1976;12:705–12.
[27] Carpinteri A. Stress-singularity and generalized fracture toughness at the vertex of re-entreant corners. Engng Fract Mech 1987;26:143–55.
[28] Joseph PF, Zhang N. Multiple root solutions, wedge paradoxes and singular stress states that are not variable-separable. Compos Sci Technol 1998;58:1839–59.
[29] Carpenter WC, Byers C. A path independent integral for computing stress intensities for v-notched cracks in a bi-material. Int J Fract 1987;35:245–68.
[30] Muller DE. A method for solving algebraic equations using an automatic computer. Math Tables Comput 1956;10:208–15.
[31] Young D, Gregory R. A survey of numerical mathematics, vol. 1. Reading (MA): Addison-Wesley; 1972.
[32] Dempsey JP, Sinclair GB. On the stress singularities in the plane elasticity of the composite wedge. J Elasticity 1979;9:373–91.
[33] Golub GH, Loan CFV. Matrix computations. 3rd ed. Baltimore: The John Hopkins University Press; 1996.
[34] Anderson E, Bai Z, Bischof C, Blackford S, Demmel J, Dongarra J, et al. LAPACK User's Guide. 3rd ed. Philadelphia: SIAM; 1999.
[35] Dundurs J. Discussion of edge-bonded dissimilar orthogonal elastic wedges under normal and shear loading. ASME J Appl Mech 1969;36:650–2.
[36] Dundurs J. Effect of elastic constants on stress in a composite under plane deformation. J Compos Mater 1967;1:310–22.
[37] Caliskan S, Karihaloo BL, Barr BIG. Study of rock-mortar interfaces. Part I: surface roughness of rock aggregates and microstructural characteristics of interface. Mag Concr Res 2002;54:449–61.
[38] Buyukoztu O, Hearing B. Crack propagation in concrete composites influenced by interface fracture parameters. Int J Solids Struct 1998;35:4055–66.
[39] Mohamed AR, Hansen W. Micromechanical modeling of crack-aggregate interaction in concrete materials. Cement Concr Compos 1999;21:349–59.
[40] Carrasquillo RL, Slate FO, Nilson AH. Microcracking and behavior of high strength concrete subject to short-term loading. ACI J 1981;78:179–86.
[41] Carpinteri A, Paggi M, Pugno N. Numerical evaluation of generalized stress-intensity factors in multi-layered composites. Int J Solids Struct 2006;43:627–41.